Jpn. J. Appl. Phys. Vol. 38 (1999) pp. 5044–5045
Part 1, No. 9A, September 1999

Short Note

Wavelength Tuning of GaAs/AlGaAs Quantum-Well Infrared Photodetectors by Thermal Interdiffusion

Xingquan LIU, Ning LI, Xiaoshuang CHEN, Wei LU, Wenlan XU, XianZhang YUAN, Na LI, S. C. SHEN, Shu YUAN[1], Hark Hoe TAN[1] and C. JAGADISH[1]

National Laboratory for Infrared Physics, Shanghai Institute of Technical Physics of Chinese Academy of Science, Shanghai 200083, P.R.China
[1]*Department of Electronic Materials Engineering, Research School of Physical Science and Engineering, The Australian National University, Canberra 0200, A.C.T., Australia*

(Received April 27, 1999; accepted for publication June 17, 1999)

Thermal interdiffusion is used to shift peak response wavelength of quantum well infrared photodetectors. A maximum 0.7 μm red-shift for 900°C annealed devices compared with as-grown one has been obtained. Error function potential profile is used to calculate the intermixing process. The large red-shift is attributed to Si-dopant enhanced intermixing. Dark current is decreased about 5 times for 900°C annealed sample than as-grown one, which is attributed to Si-dopant out-diffusion. The experimentally observed reduction in the responsivity is attributed to out-diffusion of Si-dopant and degradation of interfaces.

KEYWORDS: GaAs/AlGaAs quantum well, infrared, photodector, interdiffusion wavelength tuning

GaAs/$Al_xGa_{1-x}As$ quantum-well infrared photodetector (QWIP) has attracted extensive interest in recent years because of its promising application prospects in space remote sensing through atmospheric window region of 8–12 μm.[1–5] Compared with HgCdTe detectors, GaAs/$Al_xGa_{1-x}As$ QWIP has many advantages because of its mature materials growth technology, particularly for uniform low-cost large-area focal-plane arrays.[6–8] To adjust the detection wavelength in 8–12 μm, the well width and barrier composition can be changed. Wavelength can also be modified by post-growth intermixing of well and barrier layers. A number of means have been developed to modify the optical and electrical characteristics of quantum well structures, including ion-implantation-induced intermixing,[9,10] anodic oxidation induced intermixing,[11] thermal annealing induced intermixing[12] and cap layer induced intermixing.[13] Laser annealing induced intermixing has also been used to modify the QWIP properties recently.[14] However, laser induced intermixing will be strongly anisotropic laterally and along the growth direction because of the depth dependence and also the laser beam intensity profile. Thermal annealing induced intermixing is an effective way to get uniform modification on QWIPs.

In this work, we applied simple rapid thermal annealing induced intermixing to shift the response wavelength into the atmospheric window region which was designed out of for the as-grown devices. Important characteristics such as dark current, spectral response and responsivity were also modified.

The QWIPs are standard bound-to-quasi-continuum state transition design with peak absorption wavelength of 7.7 μm for as-grown one. The samples were grown by molecular beam epitaxy (MBE) on GaAs(100) semi-insulating substrate, including 50 periods of QWs sandwiched by 2 μm top and 1 μm bottom Si-doped (2×10^{18} cm^{-3}) GaAs contact layers. Each quantum well consisted nominally of 50 nm $Al_{0.3}Ga_{0.7}As$ barrier and 5 nm Si-doped (10^{18} cm^{-3}) GaAs well layer. Four pieces which were adjacent with each other were cleaved from the as-grown sample. Three samples (S800, S850, S900) were rapid thermally annealed (RTA) at different temperatures 800°C, 850°C and 900°C in the rapid thermal annealer for 30 s. During the annealing stage, the samples were loaded face down in contact with a fresh piece of semi-insulating GaAs wafer to prevent excessive loss of As from the surface. All samples including as-grown one were fabricated into QWIP devices. After transferring the mask pattern by lithography, $200 \times 280\,\mu m^2$ rectangular mesas were fabricated by wet etching, using 3 : 1 : 1 ($H_2O : H_2O_2 : H_3PO_4$) as the etching solution. AuGe/Ni/Au alloy was deposited and metalized as contact after the second lithography step. 45° facet was polished at the backside of the devices array before being loaded in the Dewar. Photocurrent measurement was accomplished by using the QWIPs as detectors in Bruker 113 Fourier transform Spectrometer at 80 K under different bias. To determine the modification due to thermal annealing of the QWIP devices important properties, such as dark current and responsivity were measured. Dark current was measured at 80 K during which both positive and negative bias was applied. Responsivity was measured using 500 K calibrated blackbody as infrared source under room temperature background.

Figure 1 shows the photocurrent spectra at a negative bias $V_b = -6$ V. Peak response wavelengths are 7.7 μm, 7.8 μm, 8.0 μm and 8.4 μm for as-grown, S800, S850 and S900 samples respectively. Obvious redshifts of peak response wavelength were observed in the annealed samples up to a maximum of about 0.7 μm for S900 sample. The peak response wavelength of 7.7 μm of as-grown sample was successfully shifted into the atmospheric window 8–12 μm. The magnitude of energy shifts (in wave-numbers) as a function of annealing temperature are also shown in Fig. 1. The interdiffusion is characterized by a diffusion length $L_d = (Dt)^{1/2}$, D

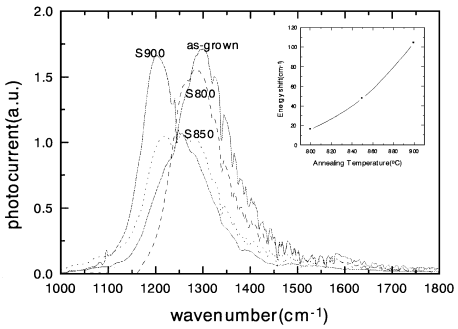

Fig. 1. Photocurrent of four samples of S800, S850, S900 for 800°C, 850°C and 900°C annealed samples and as-grown one at 80 K under the bias voltage $V_b = -6$ V. Energy shifts of different annealing temperature are also shown.

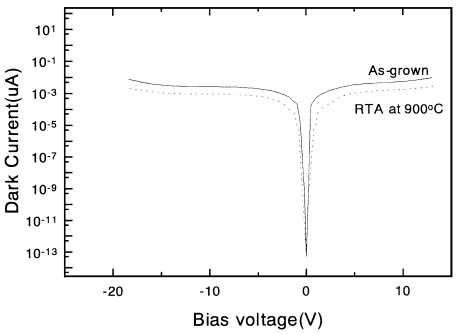

Fig. 2. Dark-current via voltage characteristics at 82 K for the as-grown device and 900°C RTA one.

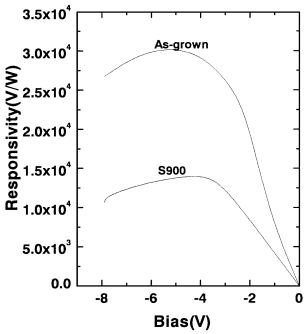

Fig. 3. The responsivity of as-grown device and 900°C annealed one.

is diffusion coefficient which is a function of annealing temperature $D = D_0 \exp(-\Delta E/kT)$ and t is the annealing time. Error function profile of Al composition was used to calculate effect of intermixing.[15] The profile of Al composition X across the quantum well interface is:

$$X(z) = X_0 \left\{ 1 - \frac{1}{2} \left[\mathrm{erf} \left[\frac{L_z + 2z}{4L_\mathrm{d}} \right] + \mathrm{erf} \left[\frac{L_z - 2z}{4L_\mathrm{d}} \right] \right] \right\} \Lambda. \quad (1)$$

Where X_0 is the Al mole fraction in the barrier and L_z is quantum well width in the as-grown structure, z is the quantization and growth direction. From eq. (1), the quantum well parameters can be obtained. Confinement potential profile of electrons in conduction band is as following:

$$U(z) = Q_\mathrm{c}[E_\mathrm{g}(z) - E_\mathrm{g}(z = 0)] \quad (2)$$

where E_g is the band gap, Q_c is the band offset splitting. Electronic subband energy can be calculated during the intermixing by using the composition profile of eq. (2). From the experimentally observed transition energy shift ΔE, we can get the corresponding diffusion length L_d by fitting the experimental results with the theoretical calculation, 0.3 nm, 0.45 nm and 0.6 nm for 800°C, 850°C and 900°C RTA devices respectively. These photocurrent measurements allow us to study sub-band energy transitions and this is a more sensitive and effective way to study the intermixing effect for the quantum well structure than the conventional way such as PL, PR etc.[9,12] By such kind of photocurrent measurement, the intermixing effect on the conduction and valence band can be studied separately.

Dark current profiles vs bias of as-grown and S900 samples were measured. The dark current of S900 was much lower than as-grown one, about a factor of 5 lower in the working bias (V_b) range ($10\,\mathrm{V} \geq |V_\mathrm{b}| \geq 2\,\mathrm{V}$ for our samples). Obvious reduction of dark current was attributed to diffusion of Si dopant (out-diffusion from well region to enhance intermixing at interface), which will consume the carriers in well. Figure 2 shows the dark current of as-grown and 900°C annealed devices. The modification of potential profile after intermixing may also contribute to the decrease of dark current, further theoretical simulation is necessary.

The responsivity at 80 K was measured from 45° incident facet using a calibrated blackbody together with a 0.6 cm diameter aperture in front of the Dewar to reduce the reflections of infrared source. The reflection losses at the Dewar window and GaAs-air interface was taken into account. The peak response was reduced by a factor of about 2 from as-grown devices as shown in Fig. 3. This decrease is due to out-diffusion of Si-dopant into barriers which will decrease the infrared absorption and this is consistent with the decrease of dark current. Also the deterioration of the interface after intermixing may also cause the degradation of devices to a certain extent.

In conclusion, without introducing any additional enhancement such as surface coating or implantation, which will introduce additional impurities or defects into the structure, we have used simple thermal annealing induced intermixing to shift the QWIP's peak response wavelength into 8–12 μm atmospheric window region. A maximum of 0.7 μm red-shift for 900°C RTA devices compared with as-grown one has been obtained. Error function potential profile was used to calculate the intermixing process. The large red-shift was attributed to Si-dopant enhanced intermixing. Dark current was decreased about 5 times for 900°C RTA sample than as-grown one, which was attributed to Si-dopant out-diffusion.

The authors would like to acknowledge the financial support by the Australian Agency for International Development (AusAID) through IDP Education Australia under Australia–China Institutional Links Program. Partial financial support by Chinese Nature Science Fund (No. 19525409) is acknowledged. XQ Liu acknowledge the financial support by Shanghai QiMingXing project, contract No. 98QA14004. SY and HHT acknowledge fellowship support from the Australian Research Council.

1) B. F. Levine, K. K. Choi, C. G. Bethea, J. Walker and R. J. Malik: Appl. Phys. Lett. **50** (1987) 1092.
2) L. S. Yu and S. S. Li: Appl. Phys. Lett. **59** (1991) 1332.
3) B. F. Levine, G. Hasnain, C. G. Bethea and N. Chand: Appl. Phys. Lett. **54** (1989) 2704.
4) B. F. Levine: J. Appl. Phys. **74** (1993) R1.
5) S. S. Li, J. Chu and Y. H. Wang: Superlattices & Microstruct. **19** (1996) 1382.
6) C. G. Bethea, B. F. Levine, M. T. Asom, R. E. Leibenguth, J. W. Stayt, K. Glogovsky, R. A. Morgan, J. D. Blackwell and W. J. Parrish: IEEE Trans. Electron Devices **40** (1993) 1957.
7) S. C. Shen: Microelectron. J. **25** (1994) 713.
8) W. Lu, H. J. Ou, M. H. Chen, X. L. Huang, S. C. Shen, R. H. Gu and L. B. Ye: Int. J. Infrared Millim. Waves **15** (1994) 137.
9) H. H. Tan, J. S. Williams, C. Jagadish, P. T. Burke and Burke and M. Gal: Appl. Phys. Lett. **68** (1996) 2401.
10) B. Elman, E. S. Koteles, P. Melman and C. A. Armiento: J. Appl. Phys. **66** (1989) 2104.
11) S. Yuan, Y. Kim, C. Jagadish, P. T. Burke, M. Gal, J. Zou, D. Q. Cai, D. J. H. Cockayne and R. M. Cohen: Appl. Phys. Lett. **70** (1997) 1269.
12) P. J. Hughes, E. H. Li and B. L. Weiss: J. Vac. Sci. Technol. B **13** (1995) 2276.
13) E. S. Koteles, B. Elman, P. Melman, J. Y. Chi and C. A. Armiento: Opt. Quantum Electron. **23** (1991) S779.
14) D. K. Sengupta, T. Horton, W. Fang, A. Curtis, J. Li, S. L. Chuang, H. Chen, M. Feng, G. E. Stiliman, A. Kar, J. Mazumder, L. Li and H. C. Liu: Appl. Phys. Lett. **70** (1997) 3573.
15) E. H. Li, B. L. Weiss and K. S. Chan: Phys. Rev. B **46** (1992) 15181.